EAST EUROPEAN JOURNAL OF PHYSICS
East Eur. J. Phys. **3**. 18-24 (2021) DOI:10.26565/2312-4334-2021-3-02

NONLINEAR CONE MODEL FOR INVESTIGATION OF RUNAWAY ELECTRON SYNCHROTRON RADIATION SPOT SHAPE†

Igor M. Pankratov[a,b,*], Volodymyr Y. Bochko[a]
[a]*V.N. Karazin Kharkiv National University, 61022 Kharkiv, Ukraine*
[b]*Institute of Plasma Physics, NSC "Kharkiv Institute of Physics and Technology" Akademichna Str.1, 61108 Kharkiv, Ukraine*
**Corresponding Author: pankratov@kipt.kharkov.ua*
Received June 16, 2021; revised July 26, 2021; accepted July 27, 2021

The runaway electron event is the fundamental physical phenomenon and tokamak is the most advanced conception of the plasma magnetic confinement. The energy of disruption generated runaway electrons can reach as high as tens of mega-electron-volt and they can cause a catastrophic damage of plasma-facing-component surfaces in large tokamaks and International Thermonuclear Experimental Reactor (ITER). Due to its importance, this phenomenon is being actively studied both theoretically and experimentally in leading thermonuclear fusion centers. Thus, effective monitoring of the runaway electrons is an important task. The synchrotron radiation diagnostic allows direct observation of such runaway electrons and an analysis of their parameters and promotes the safety operation of present-day large tokamaks and future ITER. In 1990 such diagnostic had demonstrated its effectiveness on the TEXTOR (Tokamak Experiment for Technology Oriented Research, Germany) tokamak for investigation of runaway electrons beam size, position, number, and maximum energy. Now this diagnostic is installed practically on all the present-day's tokamaks. The parameter $v_{\perp}/|v_{||}|$ strongly influences on the runaway electron synchrotron radiation behavior ($v_{||}$ is the longitudinal velocity, $v_{\perp}$ is the transverse velocity with respect to the magnetic field $\vec{B}$). The paper is devoted to the theoretical investigation of runaway electron synchrotron radiation spot shape when this parameter is not small that corresponds to present-day tokamak experiments. The features of the relativistic electron motion in a tokamak are taken into account. The influence of the detector position on runaway electron synchrotron radiation data is discussed. Analysis carried out in the frame of the nonlinear cone model. In this model, the ultrarelativistic electrons emit radiation in the direction of their velocity $\vec{v}$ and the velocity vector runs along the surface of a cone whose axis is parallel to the magnetic field $\vec{B}$. The case of the small parameter $v_{\perp}/|v_{||}|$ ($v_{\perp}/|v_{||}| \ll 1$, linear cone model) was considered in the paper: *Plasma Phys. Rep.* **22**, 535 (1996) and these theoretical results are used for experimental data analysis.
Keywords: diagnostic of runaway electrons, ultrarelativistic electrons, synchrotron radiation spot shape, nonlinear cone model, large tokamak safety operation.
PACS: 52.25.Os, 52.55.Fa, 52.70.-m

The generation of runaway electrons during disruptions poses a potential threat to the safe operation of large tokamaks. The energy of these electrons can reach as high as tens of MeV, which could lead to a serious damage of plasma-facing-component surfaces in large devices like ITER (under construction in France) (see, e. g. [1, 2]). Numerical calculations for ITER suggest about 70% of thermal current may be converted into runaway current during a disruption by avalanche mechanism [2]. Thus, effective monitoring of these high-energy runaway electrons is an emerging safety issue of the tokamak operation. The most powerful diagnostic for runaway monitoring is diagnostic based on their synchrotron radiation [3]. For the first time, this diagnostic was used in TEXTOR [4] to study the parameters of runaway electrons (beam size and position, number, and maximum energy of runaways). Now it is a routine diagnostic for present-day tokamaks: such as Joint European Torus (JET, Great Britain), Axially Symmetric Divertor Experiment (ASDEX Upgrade, Germany), DubletIII-D and Alcator C-Mod (USA), Frascati Tokamak Upgrade (FTU, Italy), *Tokamak a* Configuration Variable (TCV, Switzerland), Experimental Advanced Superconducting Tokamak (EAST, China), Korea Superconducting *Tokamak* Advanced Research (KSTAR, South Korea). The first correct theoretical analysis of the synchrotron radiation of runaway electrons with taking into account features of the relativistic electron motion in a tokamak (motion along tokamak helical magnetic field with the longitudinal velocity $v_{||}$, cyclotron gyration motion around the guiding centre with the finite transverse velocity $v_{\perp}$ with respect to the magnetic field and the vertical centrifugal drift of guiding centre motion with velocity v_{dr}) and detector position was carried out in Ref. [5] where cone model was used. Note, the finite value of parameter $v_{\perp}/|v_{||}|$ strongly influences on the runaway electron synchrotron radiation behavior but in Ref. [5] only the case of $v_{\perp}/|v_{||}| \ll 1$ was studied (linear cone model).

The highly relativistic particles emit radiation in the direction of their velocity vector [6], in this approximation, the velocity vector $\vec{v}$ runs along the surface of a cone whose axis is parallel to the magnetic field $\vec{B}$. Because of in tokamak

† ***Cite as:*** I.M. Pankratov, and V.Y. Bochko, East. Eur. J. Phys. **3**, 18 (2021), https://doi.org/10.26565/2312-4334-2021-3-02

experiments the inequality $v_\perp / |v_{||}| \gg \gamma^{-1}$ takes place, the small uncertainty introduced by the angular broadening of radiation, $\sim \gamma^{-1}$, was neglected, $\gamma = \left(1 - v^2/c^2\right)^{-1/2}$ is the relativistic factor. This model demonstrates good agreement with the full models [7]. Note that for the detailed investigation of runaway beam parameters both analysis of runaway electron synchrotron radiation spot shape and synchrotron radiation spectra must be carried out [8, 9].

NONLINEAR CONE MODEL EQUATIONS

We shall use the toroidal *(r, θ, ζ)* and Cartesian *(x, y, z)* coordinate systems, *θ* and ζ are the poloidal and toroidal angles (see Fig. 1), respectively. The tokamak confinement magnetic field was taken in the form:

$$\vec{B}(r,\vartheta) = \frac{B_{0\varsigma} R_0}{R}\left(\pm\vec{e}_\varsigma + \frac{r}{q(r)R_0}\vec{e}_\theta\right), \tag{1}$$

The circular transverse cross sections of the magnetic surfaces in a tokamak are assumed and the displacements of the magnetic surfaces relative to each other are neglected, $R = R_0 - r\cos\theta$, R_0 is the major radius of the magnetic surfaces, *q(r)* is the tokamak safety factor. The drift surfaces of runaways with small radius r_e strongly deviate from magnetic surfaces with radius *r* because of the drift shift δ_e [5]:

$$r = \sqrt{r_e^2 - \delta_e^2 \sin^2\theta} - \delta_e \cos\theta\,. \tag{2}$$

In present day tokamaks the drift orbits are shifted to low magnetic field side. The runaway electrons on the same drift surface in the low field side are located on a magnetic surface with a larger radius than electrons in the high field side.

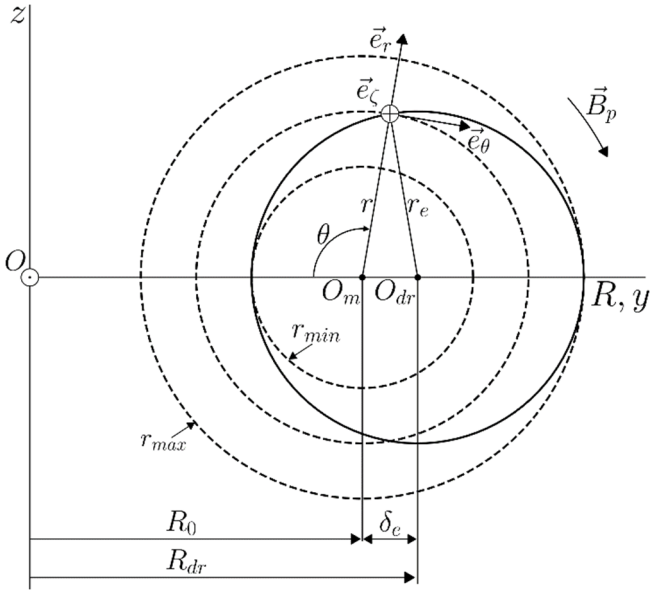

Figure 1. The cross-sections (through the plane ζ = *π/2)* of the magnetic surfaces (dashed circles) with a center at the point O_m and the drift surface with shift δ_e (solid circle) at a center O_{dr} are plotted, $r_{\min}$ and $r_{\max}$ are minimal and maximal minor radii of magnetic surfaces corresponding to this drift surface. The x-axis is directed toward the detector. The direction of the poloidal magnetic field $\vec{B}_p$ is shown.

Radiation is recorded by the detector if the condition

$$\left[\vec{v}\times\left(\vec{R}_e - \vec{Q}_{\text{det}}\right)\right] = 0 \tag{3}$$

is satisfied. In Cartesian coordinates, the radius vector of the position of the detector is represented in the next way:

$$\vec{Q}_{\text{det}} = D\vec{e}_x + Y_{\text{det}}\vec{e}_y + Z_{\text{det}}\vec{e}_z\,, \tag{4}$$

where $D > 0$ is the distance from the detector to the plane ζ = *π/2* (see Fig. 2).

Recall the main results of the linear cone model (see Ref. [5]). For the case of the small values $v_\perp/|v_{||}|$ $\left(v_\perp/|v_{||}| \ll r/q(r)R_0\right)$, when the detector is situated in the plane $z = 0$ $\left(Z_{\text{det}} = 0\right)$, the detector can record electrons for which

$$\tan\theta \approx \pm D / q(r) R_0, \tag{5}$$

i.e., the detector records electrons only from a small part of the beam cross section, which has the shape of a curved strip of varying width. If $v_\perp / |v_{||}| \gtrsim r/q(r)R_0$, the detector records a large asymmetrical spot. Note that the influence of drift orbit shift (see Eq. (2)) of high relativistic runaways on the camera record possibility is the main reason why an asymmetrical synchrotron radiation spot can be observed in present day tokamak experiments. When the large orbit shift of runaway electrons takes place, the synchrotron radiation in the low field side cannot be detected.

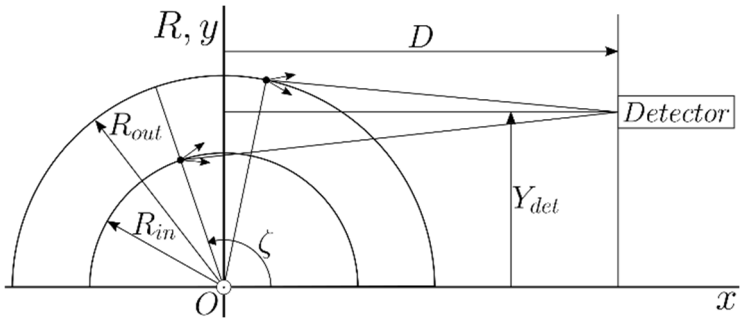

Figure 2. Relative positions of the runaway electrons beam and the detector are shown. For simplicity, case of the plane $z = 0$ and $Z_{\text{det}} = 0$ are presented, R_{in} and R_{out} are the inner and outer major radii of the beam in this plane, the cones of radiation emitted by electrons are represented schematically.

The experimental observations of runaway electron synchrotron radiation spot shape (see, e.g. [7, 9, 10, 11]) are in good agreement with the theoretical results of Ref. [5]. The observation of asymmetrical ring-like synchrotron radiation spot shape from runaway electron beams in the EAST experiments has been explained by the large orbit shift [9]. The theory of Ref. [5] may also be applied for data interpretation of a new RE diagnostic called the "Gamma Ray Imager" (GRI) which is deployed on the DIII-D tokamak [12].

In present-day tokamaks during runaway discharge the parameter $v_\perp / v_{||}$ may achieve the value of the order of 0.5 (see, e.g. [11]). The paper is devoted to the nonlinear cone model for the investigation of runaway electron synchrotron radiation spot shape in such situations. For a magnetic field with small nonuniformity it is convenient to present the electron velocity $\vec{v}$ and the radius vector $\vec{R}_e$ in the following way [13]:

$$\vec{v} = v_{||}\vec{\tau}_0 + v_\perp\left(\vec{\tau}_1 \cos\alpha + \vec{\tau}_2 \sin\alpha\right), \tag{6}$$

$$\vec{R}_e = R_0\vec{e}_R + r\vec{\tau}_1 + \frac{v_\perp}{\omega_B}\left(\vec{\tau}_1 \sin\alpha - \vec{\tau}_2 \cos\alpha\right), \tag{7}$$

where

$$\vec{e}_R = \vec{e}_x \cos\zeta + \vec{e}_y \sin\zeta, \quad \dot{\alpha} \approx \omega_B, \quad \omega_B(r,\theta) = eB(r,\theta)/\gamma m_e c \ \ (e > 0). \tag{8}$$

The right-hand triplet of the vectors is taken in the form:

$$\vec{\tau}_0 = \frac{\vec{B}}{B} = \frac{\pm\vec{e}_\zeta + (r/q(r)R_0)\vec{e}_\theta}{\sqrt{1+(r/qR_0)^2}}, \quad \vec{\tau}_1 = \left[\vec{\tau}_2 \times \vec{\tau}_0\right] = \vec{e}_r, \quad \vec{\tau}_2 = \left[\vec{\tau}_0 \times \vec{\tau}_1\right] = \frac{\pm\vec{e}_\theta - (r/q(r)R_0)\vec{e}_\zeta}{\sqrt{1+(r/qR_0)^2}}. \tag{9}$$

In tokamaks, the change of nonuniform magnetic field is small in comparison with the Larmor radius of the ultra-relativistic electron with tens of MeV energy. Hence to investigate Eqs. (3, 6, 7) the well-known asymptotic methods [13] may be used. The changes of variables (Eqs. (25.32) from Ref. [13]) are used (see appendix). With the triplet of the vectors (9) these changes of variables take the form:

$$\begin{aligned} v_{||} = \overline{v}_{||} + \frac{1}{\omega_B}\frac{\overline{v}_{||}\overline{v}_\perp}{\sqrt{1+(\overline{r}/qR_0)^2}}\left[\frac{\sin\overline{\alpha}}{\sqrt{1+(\overline{r}/qR_0)^2}}\left(\frac{\cos\overline{\theta}}{R} - \frac{\overline{r}}{(qR_0)^2}\right) \pm \frac{\cos\overline{\alpha}\sin\overline{\theta}}{R}\right] - \\ - \frac{\overline{v}_\perp^2}{4\omega_B R}\frac{\overline{r}/qR_0}{\sqrt{1+(\overline{r}/qR_0)^2}}\left[\sin 2\overline{\alpha}\sin\overline{\theta} \mp \frac{\cos 2\overline{\alpha}\cos\overline{\theta}}{\sqrt{1+(\overline{r}/qR_0)^2}}\right], \end{aligned} \tag{10a}$$

$$v_\perp = \bar{v}_\perp - \frac{1}{\omega_B}\frac{\bar{v}_\parallel^2}{\sqrt{1+(\bar{r}/qR_0)^2}}\left[\frac{\sin\bar{\alpha}}{\sqrt{1+(\bar{r}/qR_0)^2}}\left(\frac{\cos\bar{\theta}}{R}-\frac{\bar{r}}{(qR_0)^2}\right)\pm\frac{\cos\bar{\alpha}\sin\bar{\theta}}{R}\right]+$$
$$+\frac{\bar{v}_\parallel\bar{v}_\perp}{4\omega_B R}\frac{\bar{r}/qR_0}{\sqrt{1+(\bar{r}/qR_0)^2}}\left[\sin 2\bar{\alpha}\sin\bar{\theta}\mp\frac{\cos 2\bar{\alpha}\cos\bar{\theta}}{\sqrt{1+(\bar{r}/qR_0)^2}}\right], \tag{10b}$$

$$\alpha = \bar{\alpha} - \frac{1}{\omega_B}\frac{1}{\sqrt{1+(\bar{r}/qR_0)^2}}\left\{\mp\frac{\bar{v}_\parallel^2}{\bar{v}_\perp}\frac{\sin\bar{\alpha}\sin\bar{\theta}}{R}+\frac{1}{\bar{v}_\perp}\frac{\cos\bar{\alpha}}{\sqrt{1+(\bar{r}/qR_0)^2}}\left[\bar{v}_\parallel^2\left(\frac{\cos\bar{\theta}}{R}-\frac{\bar{r}}{(qR_0)^2}\right)-\bar{v}_\perp^2\left(\frac{1}{\bar{r}}-\frac{(\bar{r}/qR_0)^2\cos\bar{\theta}}{R}\right)\right]\right\}+$$
$$+\frac{\bar{v}_\parallel}{4\omega_B R}\frac{\bar{r}/qR_0}{\sqrt{1+(\bar{r}/qR_0)^2}}\left[\cos 2\bar{\alpha}\sin\bar{\theta}\pm\frac{\sin 2\bar{\alpha}\cos\bar{\theta}}{\sqrt{1+(\bar{r}/qR_0)^2}}\right]-\frac{\bar{v}_\perp}{\omega_B R}\left[\cos\bar{\theta}\cos\bar{\alpha}\mp\frac{\sin\bar{\theta}\sin\bar{\alpha}}{\sqrt{1+(\bar{r}/qR_0)^2}}\right]- \tag{10c}$$
$$-\frac{\bar{v}_\perp}{\omega_B qR_0}\frac{\bar{r}/qR_0}{1+(\bar{r}/qR_0)^2}\cos\bar{\alpha}.$$

Here averaging of variables is determined in the usual way: $\bar{f} = (1/2\pi)\int_0^{2\pi} f d\alpha$.

For simplicity below the line over averaged variables is omitted. After substitutions of these changes of variables (10a, b, c) in Eq. (6) the components of electron velocity take the form:

$$v_x = \cos\Delta\left[\mp v_\parallel + v_\perp\frac{r}{qR_0}\sin\alpha-\frac{v_\parallel^2}{\omega_B R}\frac{r}{qR_0}\cos\theta-\frac{v_\parallel v_\perp}{\omega_B R}\sin(\theta\pm\alpha)\pm\frac{v_\parallel v_\perp}{\omega_B qR_0}\frac{r}{qR_0}\sin\alpha+\frac{v_\perp^2}{\omega_B qR_0}\cos^2\alpha\right]+$$
$$+\sin\Delta\left[-v_\parallel\frac{r}{qR_0}\sin\theta+v_\perp\cos(\theta\pm\alpha)\mp\frac{v_\parallel^2}{\omega_B qR_0}\frac{r}{qR_0}\sin\theta\mp\frac{v_\parallel v_\perp}{\omega_B R}\frac{r}{qR_0}\sin(\theta\pm\alpha)\sin\theta\mp\frac{v_\parallel v_\perp}{4\omega_B R}\frac{r}{qR_0}\cos\alpha\mp\right. \tag{11a}$$
$$\left.\mp\frac{v_\perp^2}{\omega_B r}\sin(\theta\pm\alpha)\cos\alpha\pm\frac{v_\perp^2}{\omega_B R}\cos(\theta\pm\alpha)\sin(\theta\pm\alpha)\right],$$

$$v_y = \cos\Delta\left[v_\parallel\frac{r}{qR_0}\sin\theta-v_\perp\cos(\theta\pm\alpha)\pm\frac{v_\parallel^2}{\omega_B qR_0}\frac{r}{qR_0}\sin\theta\pm\frac{v_\parallel v_\perp}{\omega_B R}\frac{r}{qR_0}\sin(\theta\pm\alpha)\sin\theta\pm\frac{v_\parallel v_\perp}{4\omega_B R}\frac{r}{qR_0}\cos\alpha\pm\right.$$
$$\left.\pm\frac{v_\perp^2}{\omega_B r}\sin(\theta\pm\alpha)\cos\alpha\mp\frac{v_\perp^2}{\omega_B R}\cos(\theta\pm\alpha)\sin(\theta\pm\alpha)\right]+ \tag{11b}$$
$$+\sin\Delta\left[\mp v_\parallel + v_\perp\frac{r}{qR_0}\sin\alpha-\frac{v_\parallel^2}{\omega_B R}\frac{r}{qR_0}\cos\theta-\frac{v_\parallel v_\perp}{\omega_B R}\sin(\theta\pm\alpha)\pm\frac{v_\parallel v_\perp}{\omega_B qR_0}\frac{r}{qR_0}\sin\alpha+\frac{v_\perp^2}{\omega_B qR_0}\cos^2\alpha\right],$$

$$v_z = v_\parallel\frac{r}{qR_0}\cos\theta+v_\perp\sin(\theta\pm\alpha)\mp\frac{v_\parallel^2+0.5v_\perp^2}{\omega_B R}\pm\frac{v_\parallel^2}{\omega_B qR_0}\frac{r}{qR_0}\cos\theta\pm\frac{v_\parallel v_\perp}{\omega_B R}\frac{r}{qR_0}\sin(\theta\pm\alpha)\cos\theta\pm\frac{v_\parallel v_\perp}{4\omega_B R}\frac{r}{qR_0}\sin\alpha$$
$$\mp\frac{v_\perp^2}{2\omega_B R}\cos 2(\theta\pm\alpha)\pm\frac{v_\perp^2}{\omega_B r}\cos(\theta\pm\alpha)\cos\alpha \tag{11c}$$

and components of coordinates (from Eq. (7)):

$$X_e = -\left(R_0 - r\cos\theta\right)\sin\Delta,\quad Y_e = \left(R_0 - r\cos\theta\right)\cos\Delta,\quad Z_e = r\sin\theta\mp\frac{v_\perp}{\omega_B}\cos\left(\theta\pm\alpha\right), \tag{12}$$

where $\zeta = \pi/2+\Delta$. The terms that are proportional to small parameter $(r/q(r)R_0)^2 << 1$ are omitted.

By inserting equations 11(a, b, c) and 12 into Eq. (3), the expressions that allow analysis of the synchrotron radiation emitted by runaway electrons in tokamaks are obtained ($v_\perp/|v_\parallel| >> r/q(r)R_0$). From expression

$$(Z_e - Z_{\text{det}})v_x = \left(X_e - D\right)v_z \tag{13}$$

we get:

$$\pm\left[r\sin\theta\mp\frac{v_\perp}{\omega_B}\cos\left(\theta\pm\alpha\right)-Z_{\text{det}}\right]\left[\cos\Delta\mp\sin\Delta\frac{v_\perp}{v_\parallel}\cos\left(\theta\pm\alpha\right)\right]=$$
$$=\left[D+\left(R_0-r\cos\theta\right)\sin\Delta\right]\left[\frac{r}{qR_0}\cos\theta+\frac{v_\perp}{v_\parallel}\sin\left(\theta\pm\alpha\right)\mp\frac{1}{v_\parallel}\frac{v_\parallel^2+0.5v_\perp^2}{\omega_B R_0}\pm\frac{v_\perp}{v_\parallel}\frac{v_\perp}{\omega_B r}\cos\left(\theta\pm\alpha\right)\cos\alpha\right]. \tag{14}$$

From expression

$$\left(X_e-D\right)v_y=\left(Y_e-Y_{\text{det}}\right)v_x \tag{15}$$

we get:

$$\sin\Delta\left[1\pm\frac{Y_{\text{det}}}{D}\frac{v_\perp}{v_\parallel}\cos\left(\theta\pm\alpha\right)\right]=\frac{Y_{\text{det}}\cos\Delta-\left(R_0-r\cos\theta\right)}{D}\mp\cos\Delta\frac{v_\perp}{v_\parallel}\cos\left(\theta\pm\alpha\right). \tag{16}$$

In Eqs. (14) and (16) the small terms that are of the order of $(v_{||}{}^2/\omega_B qR_0)(r/qR_0)$, $(v_{||}v_\perp/\omega_B qR)(r/qR_0)$ and $v_\perp{}^2/\omega_B R$ are omitted. The solution of Eq. (16) has the next form:

$$\cos\Delta=\frac{\left[1\pm\frac{Y_{\text{det}}}{D}\frac{v_\perp}{v_\parallel}\cos\left(\theta\pm\alpha\right)\right]\left\{\left[1+\left(Y_{\text{det}}/D\right)^2\right]\left[1+\left(v_\perp/v_\parallel\right)^2\cos^2\left(\theta\pm\alpha\right)\right]-\left(R/D\right)^2\right\}^{1/2}+\left(\frac{R}{D}\right)\left[\frac{Y_{\text{det}}}{D}\mp\frac{v_\perp}{v_\parallel}\cos\left(\theta\pm\alpha\right)\right]}{\left[1+\left(Y_{\text{det}}/D\right)^2\right]\left[1+\left(v_\perp/v_\parallel\right)^2\cos^2\left(\theta\pm\alpha\right)\right]}, \tag{17}$$

$$\sin\Delta=\frac{\left[\frac{Y_{\text{det}}}{D}\mp\frac{v_\perp}{v_\parallel}\cos\left(\theta\pm\alpha\right)\right]\left\{\left[1+\left(Y_{\text{det}}/D\right)^2\right]\left[1+\left(v_\perp/v_\parallel\right)^2\cos^2\left(\theta\pm\alpha\right)\right]-\left(R/D\right)^2\right\}^{1/2}-\left(\frac{R}{D}\right)\left[1\pm\frac{Y_{\text{det}}}{D}\frac{v_\perp}{v_\parallel}\cos\left(\theta\pm\alpha\right)\right]}{\left[1+\left(Y_{\text{det}}/D\right)^2\right]\left[1+\left(v_\perp/v_\parallel\right)^2\cos^2\left(\theta\pm\alpha\right)\right]}. \tag{18}$$

The synchrotron radiation of runaway electron may be detected by the camera only if the next inequality holds (solution of Eqs, (17), (18) exists):

$$\left[1+\left(Y_{\text{det}}/D\right)^2\right]\left[1+\left(v_\perp/v_\parallel\right)^2\cos^2\left(\theta\pm\alpha\right)\right]\geq\left(R/D\right)^2. \tag{19}$$

DISCUSSIONS

For $v_\perp/|v_{||}|\ll 1$ the equations (14, 16) correspond to the linear cone model equations of Ref. [5]:

$$\pm\left(r\sin\theta-Z_{\text{det}}\right)\approx\left[\frac{r}{qR_0}\cos\theta+\frac{v_\perp}{v_\parallel}\sin\left(\theta\pm\alpha\right)\mp\frac{1}{v_\parallel}\frac{v_\parallel^2+0.5v_\perp^2}{\omega_B R_0}\right]\left(D+R\sin\Delta\right), \tag{20}$$

$$\sin\Delta\approx\pm\frac{r}{qR_0}\sin\theta\mp\frac{v_\perp}{v_\parallel}\cos\left(\theta\pm\alpha\right)+\frac{Y_{\text{det}}-R}{D},\quad\cos\Delta\approx 1. \tag{21}$$

The upper signs in the equations of the paper correspond to the case when the magnetic field $\vec{B}$ is directed away from the detector, and for the lower sign field is directed toward the detector. For the electron moving toward the detector the longitudinal velocity $v_\parallel$ is negative for upper sign ($v_\parallel<0$) and positive for lower sign ($v_\parallel>0$). Hence:

$$\cos\Delta=\frac{\left[1-\frac{Y_{\text{det}}}{D}\frac{v_\perp}{|v_\parallel|}\cos\left(\theta\pm\alpha\right)\right]\left\{\left[1+\left(Y_{\text{det}}/D\right)^2\right]\left[1+\left(v_\perp/v_\parallel\right)^2\cos^2\left(\theta\pm\alpha\right)\right]-\left(R/D\right)^2\right\}^{1/2}+\left(\frac{R}{D}\right)\left[\frac{Y_{\text{det}}}{D}+\frac{v_\perp}{|v_\parallel|}\cos\left(\theta\pm\alpha\right)\right]}{\left[1+\left(Y_{\text{det}}/D\right)^2\right]\left[1+\left(v_\perp/v_\parallel\right)^2\cos^2\left(\theta\pm\alpha\right)\right]}, \tag{22}$$

$$\sin\Delta=\frac{\left[\frac{Y_{\text{det}}}{D}+\frac{v_\perp}{|v_\parallel|}\cos\left(\theta\pm\alpha\right)\right]\left\{\left[1+\left(Y_{\text{det}}/D\right)^2\right]\left[1+\left(v_\perp/v_\parallel\right)^2\cos^2\left(\theta\pm\alpha\right)\right]-\left(R/D\right)^2\right\}^{1/2}-\left(\frac{R}{D}\right)\left[1-\frac{Y_{\text{det}}}{D}\frac{v_\perp}{|v_\parallel|}\cos\left(\theta\pm\alpha\right)\right]}{\left[1+\left(Y_{\text{det}}/D\right)^2\right]\left[1+\left(v_\perp/v_\parallel\right)^2\cos^2\left(\theta\pm\alpha\right)\right]}. \tag{23}$$

First situation when $Y_{det}/D > 1$ is considered. If $1-(Y_{det}/D)(v_\perp/|v_\parallel|)\cos(\theta\pm\alpha)\geq 0$, then $\cos\Delta\geq 0$ and

$$\sin\Delta\geq 0, \text{ if } \left[(Y_{det}/D)+(v_\perp/|v_{||}|)\cos(\theta\pm\alpha)\right]^2\geq (R/D)^2, \tag{24}$$

$$\sin\Delta\leq 0, \text{ if } \left[(Y_{det}/D)+(v_\perp/|v_{||}|)\cos(\theta\pm\alpha)\right]^2\leq (R/D)^2. \tag{25}$$

If $1-(Y_{det}/D)(v_\perp/|v_\parallel|)\cos(\theta\pm\alpha)\leq 0$, then $\sin\Delta\geq 0$ and

$$\cos\Delta\geq 0, \text{ if } \left[(Y_{det}/D)(v_\perp/|v_{||}|)\cos(\theta\pm\alpha)-1\right]^2\leq (R/D)^2, \tag{26}$$

$$\cos\Delta\leq 0, \text{ if } \left[(Y_{det}/D)(v_\perp/|v_{||}|)\cos(\theta\pm\alpha)-1\right]^2\geq (R/D)^2. \tag{27}$$

Second situation is when $Y_{det}/D < 1$. If $(Y_{det}/D)+(v_\perp/|v_\parallel|)\cos(\theta\pm\alpha)\geq 0$, then $\cos\Delta\geq 0$ and $\sin\Delta\geq 0$ or $\sin\Delta\leq 0$ if inequality (24) or (25) holds, respectively.

If $(Y_{det}/D)+(v_\perp/|v_\parallel|)\cos(\theta\pm\alpha)\leq 0$, then $\sin\Delta\leq 0$ and $\cos\Delta\geq 0$ or $\cos\Delta\leq 0$ if inequality (27) or (26) holds, respectively.

In Eqs. (14), (16) the parameter $v_\perp/|v_{||}|$ is not small, the solution of Eq. (14) exists only if $|\sin(\theta\pm\alpha)|\ll 1$ and $|\cos(\theta\pm\alpha)|\approx 1$ ($r \ll D$, $Z_{det}\sim r$). Very important conclusion: for each poloidal angle θ the synchrotron radiation of runaway electron is detected by the camera for certain values of α only.

CONCLUSIONS

The analytical expressions that allow analysis of the synchrotron radiation emitted by runaway electrons in tokamaks have been obtained, the finite ratio $v_\perp/v_{||}$ the order of 0.5, the tokamak safety factor *q(r),* the horizontal displacement δ_e of the drift surfaces of electrons with respect to the magnetic surfaces, and the position of the detector are taken into account. This situation corresponds to present-day tokamak runaway electron experiments.

It has been shown that besides the parameter $v_\perp/|v_{||}|$, the ratio Y_{det}/D is also a key parameter for the analysis of the synchrotron radiation spot shape. It should be noted that for each poloidal angle θ the synchrotron radiation of runaway electron is detected by the camera for certain values of α (cyclotron rotation angle) only.

APPENDIX

For readers convenience the equations that corresponds to Eqs. 25.32 of Ref. 13 are presented:

$$\begin{aligned} v_\parallel &= \overline{v}_\parallel + \frac{\overline{v}_\parallel\overline{v}_\perp}{\omega_B}\left[\vec{\tau}_1(\vec{\tau}_0\nabla)\vec{\tau}_0\sin\overline{\alpha}-\vec{\tau}_2(\vec{\tau}_0\nabla)\vec{\tau}_0\cos\overline{\alpha}\right]+ \\ &+\frac{\overline{v}_\perp^2}{4\omega_B}\left\{\left[\vec{\tau}_1(\vec{\tau}_1\nabla)\vec{\tau}_0-\vec{\tau}_2(\vec{\tau}_2\nabla)\vec{\tau}_0\right]\sin 2\overline{\alpha}-\left[\vec{\tau}_1(\vec{\tau}_2\nabla)\vec{\tau}_0+\vec{\tau}_2(\vec{\tau}_1\nabla)\vec{\tau}_0\right]\cos 2\overline{\alpha}\right\}, \end{aligned} \tag{A1}$$

$$\begin{aligned} v_\perp &= \overline{v}_\perp + \frac{\overline{v}_\parallel^2}{\omega_B}\left[\vec{\tau}_2(\vec{\tau}_0\nabla)\vec{\tau}_0\cos\overline{\alpha}-\vec{\tau}_1(\vec{\tau}_0\nabla)\vec{\tau}_0\sin\overline{\alpha}\right]+ \\ &+\frac{\overline{v}_\parallel\overline{v}_\perp}{4\omega_B}\left\{\left[\vec{\tau}_1(\vec{\tau}_2\nabla)\vec{\tau}_0+\vec{\tau}_2(\vec{\tau}_1\nabla)\vec{\tau}_0\right]\cos 2\overline{\alpha}-\left[\vec{\tau}_1(\vec{\tau}_1\nabla)\vec{\tau}_0-\vec{\tau}_2(\vec{\tau}_2\nabla)\vec{\tau}_0\right]\sin 2\overline{\alpha}\right\}, \end{aligned} \tag{A2}$$

$$\begin{aligned} \alpha &= \overline{\alpha}-\frac{1}{\omega_B}\left\{\frac{1}{\overline{v}_\perp}\left[\overline{v}_\parallel^2\vec{\tau}_1(\vec{\tau}_0\nabla)\vec{\tau}_0-\overline{v}_\perp^2\vec{\tau}_2(\vec{\tau}_2\nabla)\vec{\tau}_1\right]\cos\overline{\alpha}-\frac{1}{\overline{v}_\perp}\left[\overline{v}_\perp^2\vec{\tau}_1(\vec{\tau}_1\nabla)\vec{\tau}_2-\overline{v}_\parallel^2\vec{\tau}_2(\vec{\tau}_0\nabla)\vec{\tau}_0\right]\sin\overline{\alpha}\right\}- \\ &-\frac{\overline{v}_\parallel}{4\omega_B}\left\{\left[\vec{\tau}_1(\vec{\tau}_1\nabla)\vec{\tau}_0-\vec{\tau}_2(\vec{\tau}_2\nabla)\vec{\tau}_0\right]\cos 2\overline{\alpha}+\left[\vec{\tau}_1(\vec{\tau}_2\nabla)\vec{\tau}_0+\vec{\tau}_2(\vec{\tau}_1\nabla)\vec{\tau}_0\right]\sin 2\overline{\alpha}\right\}-\frac{\overline{v}_\perp}{\omega_B^2}\left(\vec{\tau}_1\cos\overline{\alpha}+\vec{\tau}_2\sin\overline{\alpha}\right)\nabla\omega_B, \end{aligned} \tag{A3}$$

$$\vec{R}_e = R_0\vec{e}_R+\overline{r}\vec{\tau}_1+\frac{\overline{v}_\perp}{\omega_B}\left(\vec{\tau}_1\sin\overline{\alpha}-\vec{\tau}_2\cos\overline{\alpha}\right). \tag{A4}$$

ORCID IDs
Igor M. Pankratov, https://orcid.org/0000-0001-5876-4618; **Volodymyr Y. Bochko**, https://orcid.org/0000-0003-2109-968X

REFERENCES

[1] B.N. Breizman, P. Aleynikov, E.M. Hollmann, and M. Lehnen, Nuclear Fusion, **59**, 083001 (2019), https://doi.org/10.1088/1741-4326/ab1822
[2] T.C. Hender, J.C. Wesley, J. Bialek, A. Bondeson, A.H. Boozer, R.J. Buttery, A. Garofalo, et al. Nuclear Fusion, **47,** 128 (2007), https://doi.org/10.1088/0029-5515/47/6/S03
[3] R. Jaspers, N.J. Lopes Cardozo, A.J.H. Donne, H.L.M. Widdershoven, and K.H. Finken, Review Sci. Instruments, **72-II**, 466 (2001), https://doi.org/10.1063/1.1318245
[4] K.H. Finken, J.G. Watkins, D. Rusbuldt, W.J. Corbett, K.H. Dippel, D.M. Goebel, and R.A. Moyer, Nuclear Fusion, **30**, 859 (1990), https://doi.org/10.1088/0029-5515/30/5/005
[5] I.M. Pankratov, Plasma Physics Reports, **22**, 535 (1996), https://www.researchgate.net/profile/Igor-Pankratov/publication/252431545_Analysis_of_the_synchrotron_radiation_emitted_by_runaway_electrons/links/0deec52c98ac368d5c000000/Analysis-of-the-synchrotron-radiation-emitted-by-runaway-electrons.pdf
[6] L.D. Landau, and E.M. Lifshitz, *The classical theory of fields* (Pergamon press).
[7] M. Hoppe O. Embréus, R.A. Tinguely, R.S. Granetz, A. Stahl, and T. Fülöp, Nuclear Fusion **58**, 026032 (2018), https://doi.org/10.1088/1741-4326/aa9abb
[8] I.M. Pankratov, Plasma Physics Reports, **25**, 145 (1999), https://inis.iaea.org/search/search.aspx?orig_q=RN:35003886
[9] R.J. Zhou, I.M. Pankratov, L.Q. Hu, M. Xu, and J.H. Yang, Physics of Plasmas, **21**, 063302 (2014), https://doi.org/10.1063/1.4881469
[10] I. Entrop, R. Jaspers, N.J.L. Cardozo, and K.H. Finken, Plasma Physics and Controlled Fusion, **41**, 377 (1999), https://doi.org/10.1088/0741-3335/41/3/004
[11] J.H. Yu, E.M. Hollmann, N. Commaux, N.W. Eidietis, D.A. Humphreys, A.N. James, T.C. Jernigan, and R.A. Moyer, Physics of Plasmas, **20**, 042113 (2013), https://doi.org/10.1063/1.4801738
[12] C. Paz-Soldan, C.M. Cooper, P. Aleynikov, N.W. Eidietis, A. Lvovskiy, D.C. Pace, D.P. Brennan, E.M. Hollmann, C. Liu, R.A. Moyer, and D. Shiraki, Physics of Plasmas, **25**, 056105 (2018), https://doi.org/10.1063/1.5024223
[13] N.N. Bogoliubov, Y.A. Mitropolsky, *Asymptotic methods in theory of non-linear oscillations* (Gordon and Breach Science Publishers, 1961).

ДОСЛІДЖЕННЯ ФОРМИ ПЛЯМИ СИНХРОТРОННОГО ВИПРОМІНЮВАННЯ ЕЛЕКТРОНІВ-ВТІКАЧІВ В МОДЕЛІ ВИПРОМІНЮВАННЯ СПРЯМОВАНОГО УЗДОВЖ ПОВЕРХНІ КОНУСА ЇХ ШВИДКОСТЕЙ

І.М. Панкратов[a,b], В.Ю. Бочко[a]
[a]Харківський національний університет імені В.Н. Каразіна, м. Свободи 4, 61022 Харків, Україна
[b]Інститут фізики плазми, ННЦ "Харківський фізико-технічний інститут"
вул. Академічна 1, 61108 Харків, Україна

Електрони-втікачі – це фундаментальне фізичне явище, а токамак – найбільш просунута концепція магнітного утримання плазми. Енергія електронів-втікачів, які утворюються під час зривів розряду, може досягати десятків мегаелектронвольт, потрапляння яких на конструкційні елементи сучасних великих токамаків і споруджуваного міжнародного токамака-реактора ITER може призвести до катастрофічних наслідків. Внаслідок актуальності, дане явище активно досліджується як теоретично, так і експериментально у провідних термоядерних центрах. Ефективний моніторинг електронів-втікачів є важливою задачею. Діагностика, що базується на синхротронному випромінюванні електронів-втікачів, дозволяє як безпосереднє їх спостереження, так і аналіз параметрів цих електронів, що сприяє безпечній роботі сучасних токамаків та майбутнього токамаку-реактора ITER. В 1990 році дана діагностика показала свою ефективність на токамаці TEXTOR для дослідження радіусу пучка, розташування, кількості та максимальної енергії електронів-втікачів. Ця діагностика встановлена на більшості сучасних токамаків. Параметр $v_\perp/|v_{||}|$ виявляє сильний вплив на поведінку синхротронного випромінювання електронів-втікачів ($v_{||}$ - поздовжня, а $v_\perp$ - поперечна швидкість по відношенню до магнітного поля $\vec{B}$). В статті теоретично вивчається форма плями синхротронного випромінювання електронів-втікачів, коли цей параметр не малий, що відповідає теперішнім експериментам на токамаках. Враховані особливості руху релятивістського електрона в токамаці. Проаналізовано вплив розташування детектора на спостереження синхротронного випромінювання електронів – втікачів. Аналіз проведено у межах нелінійної моделі поверхні «конуса швидкостей». В цій моделі випромінювання ультрарелятивістських електронів спрямовано уздовж вектору їх швидкості $\vec{v}$, а вектор швидкості спрямовано уздовж поверхні конуса з віссю паралельній магнітному полю $\vec{B}$. Раніше випадок малого параметру $v_\perp/|v_{||}|$ ($v_\perp/|v_{||}| \ll 1$, лінійна модель) розглянуто в статті: Физика плазмы, **22**, 588 (1996), ці теоретичні результати використовуються для аналізу експериментальних даних.

Ключові слова: діагностика електронів-втікачів, ультрарелятивістські електрони, форма плями синхротронного випромінювання, нелінійна модель поверхні конуса швидкостей, безпека роботи токамака.